

Laboratory simulation of vibration effects met at vehicular road transportation of fruits and vegetables

C.L. Ranatunga^{1*}, H.H.E Jayaweera², S.K.K Suraweera² and T.R. Ariyaratne²

1. Dept of Physics, Faculty of Applied Sciences, University of Sri Jayewardenepura, Nugegoda, Sri Lanka

2. Centre for Instrument Development, Department of Physics, Faculty of Science, University of Colombo, Colombo 03, Sri Lanka

**Corresponding author*

Received on : 01-07-2013

Accepted on: 05-08-2013

Abstract

For studying and controlling the vibration effects present at vehicular road transportation, the quantitative estimation and laboratory simulation of the same becomes vital. Using an accelerometer, the vibration acceleration was measured in terms of power spectral density (PSD) in dB/Hz unit. Average of the maximum vertical vibration (PSDmax) levels produced by the truck over the time of experiment were 0.005 dB/Hz, 0.01 dB/Hz and 0.05 dB/Hz at the front, middle and rear of the truck-bed respectively. Vertical vibration acceleration levels present at actual vehicular road transportation were simulated at the laboratory using a fabricated electrodynamic vibrator. PSDmax levels met at the actual road transportation by truck were simulated at the laboratory by varying the eccentric mass and the loaded-weight of the vibrator. Eccentric mass adjusted in between 200 g and 300 g permits generation of PSDmax levels of interest on the vibrator at no-load. Loading a weight in the range from 15 kg to 60 kg allows generation of the required PSDmax levels when the eccentric mass is set to 400 g. By adjusting mutually the eccentric mass and the loaded-weight, the vibrator is capable of simulating the PSDmax levels of the interest.

Keywords: Vibration sensor, Accelerometer, Vibration simulator, Vehicular vibration, Fruit quality degradation

Introduction

Vibration effects inflict damage on commodities during their transportation. Damage appears as a degradation of the quality of the commodity, immediately after or sometimes later, in the course of transportation. Fresh fruits and vegetables are living organisms.

Their quality is largely affected by numerous customs used in post-harvest handling. Method used in harvesting (mechanical or manual), collecting, packing, transporting and storing may cause visible or, very often invisible, damages into the interior of the fruit or vegetable. Dynamic forces during fruit transport and handling cause by far the most bruise damage. One such aspect of quality is the detrimental effect of impact damage. This is not restricted to visual aspects, but higher risk of bacterial and fungal contamination, leading to a lower shelf-life, also results from this damage. Other collateral effects include water loss from the fruit. For most fruit types, bruising is the most common type of post-harvest mechanical injury. The vibration component of the vehicle with the largest effect during the vehicular road transportation is the vertical vibration because the vibration component in the vertical direction is greater than the others (Vursavus and Ozguven, 2004). For the study of the damages inflicted to fruits & vegetables due to transport vibration, it is essential to estimate the effective vibration levels quantitatively. Also the laboratory simulation of the vibration levels experienced at the actual vehicular road transportation would facilitate study and control of the effect of vibration on the transport commodity.

Vibration sensing

Accelerometers are widely used as the sensor for vibration acceleration. Piezoelectric micro accelerometers have been employed in evaluation of the vibration damage to loquats and pears during transportation (Barchi et al., 2002, Berardinelli et al., 2005, Slaughter et al., 1993, Zhou et al., 2007). Calibration of road roughness meters, estimation of the vibration effects of portable electricity generators, evaluation of the comfort of tractor and heavy vehicle driver's seat—(Cann et al., 2004) are a few of other areas where accelerometers are widely used. Battery-operated tri axial accelerometers have been used in vibration detection in fruit & vegetable transportation in Japan—(Ishikawa et al., 2009) and in Thailand (Chonhenchob et al., 2009). Of the piezoelectric and capacitive type accelerometers, the latter are low-cost and, have good linearity and high output stability. They are ideal for on-board applications where acceleration levels are low.

Vertical vibration acceleration at road transportation by truck

Chonhenchob et.al. in 2009 has shown that the most prominent frequencies in truck transportation was found between 5 to 7 Hz. They have also shown that in the higher frequency range, the vertical vibration levels for truck highway transportation were much lower. In the study on simulated in-transit vibration damage to grapes and strawberries, Fisher et.al. in 1992 have concentrated to the frequency range from 5 to 10 Hz (Fischer et al., 1992). In the study of cherry transportation by truck from Yamagata to Taipei, Ishikawa et.al. have observed peak vibration acceleration at 15 Hz in Japan but at lower frequencies from 2 to 3 Hz in Taiwan—(Ishikawa et al., 2009). Van Zeebroeck et.al. in 2006 have stated the significance of the vibration acceleration level in between 1 to 5 Hz in their study on damages occurred during apple transportation by steel spring trucks.

Further, Vursavus & Ozguven in 2004 have pointed out in their research on mechanical damage inflicted to apples during transportation that, out of the entire frequency range from 3 to 200 Hz present on the truck bed, only the frequencies between 5 Hz to 10 Hz imparts significant vibration effects. In their study, within this critical frequency region, the rear side produces nearly 8 to 10 times higher vibration energy compared to the middle and front sides of the empty truck.

Vibration simulation

The best method for studying the damages inflicted on fresh produce during truck transportation is to work with the real situations i.e. the operations in the actual road transportation of fruit bins by trucks. However, due to the difficulties arising with controlling the experimental conditions in the actual transportation, it is customary to simulate the vibration environment in the laboratory (Vursavus and Ozguven, 2004). Though the actual vibration is a combination of random and sinusoidal patterns, a sinusoidal vibration simulator had been used for the simulated transport because of the limitations of the vibrator performance (Usuda et al., 2008). In an electro-dynamic vibrator an eccentric mass is set to rotate about the axis. Distance to the eccentric mass from the central axis and the magnitude of the mass determines the effect of the vibration acceleration. Different vibration accelerations and different frequencies can be achieved by varying the size and angular velocity of the rotating mass. Acceleration levels are expressed as a plot of acceleration spectral density (ASD) or power spectral density (PSD) vs. frequency. The square root of the area under the curve is the root mean square acceleration g_{rms} (Pauly, 2008).

To distinguish the gravitational acceleration due to free fall from the simple acceleration due to rate of change of velocity, the unit g is often used. One g is the acceleration due to gravity of Earth's surface and is the standard gravity g_n which is defined as 9.80665 ms^{-2} . A typical person can handle about 5 g of acceleration before losing consciousness.

Materials and methods

Vibration sensing

Steval MKi006V1 evaluation kit based on LIS302DL 3-axis linear MEMS accelerometer (capacitive) was used for the estimation of vibration acceleration in terms of Power Spectral Density (PSD) in this investigation. This accelerometer is a low-power, tri-axis device with pulse-width modulation (PWM) output and, is powered by the computer's USB connection itself. Hence it permits longer un-interrupted operation without drop of voltage during long truck journeys. In the output signal with PWM, the length of time the voltage is high will be proportional to the magnitude of acceleration. At the USB port it is fed to the computer as a 8-bit digital value in 2's complement format. Bandwidth of the accelerometer is the frequency that a reliable reading is obtainable. For slow-moving tilt applications, a bandwidth of 50 Hz will probably suffice. For vibration measurements it requires a higher bandwidth. This particular accelerometer has a data rate of 100 Hz and a maximum swing of $\pm 2 g$ acceleration level (Steval, 2006).

Calibration of accelerometers and their orientation

A tri-axis accelerometer reads acceleration data \underline{l} , \underline{m} and \underline{n} , where \underline{l} , \underline{m} and \underline{n} are magnitudes of acceleration measured in ADC units along three axes x , y and z respectively (see Figure 1). \underline{l} , \underline{m} and \underline{n} are the acceleration data converted to 2's complement in sign and magnitude (ADC values). The orientation of one of the three axes accurately to the vertical (or horizontal) direction and maintaining it throughout the vibration analysis is difficult. However, with the knowledge of the directional cosines, the angle a , b and c , between each axis and the "vertical" direction along with the acceleration due to gravity (g) could be obtained as follows.

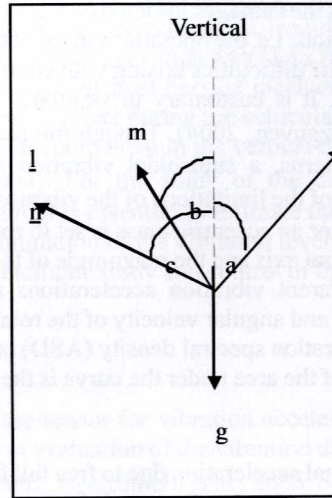


Figure 1. Angles a , b and c subtended with vertical by the three axes at an arbitrary positioning of the accelerometer

When K is the variation of the acceleration per unit ADC value,

$$g \cos a = kl ; \quad a = \cos^{-1} \left(\frac{kn}{g} \right) \quad \dots\dots\dots(1)$$

$$g \cos b = km ; \quad b = \cos^{-1} \left(\frac{km}{g} \right) \quad \dots\dots\dots(2)$$

$$g \cos c = kn ; \quad c = \cos^{-1} \left(\frac{kn}{g} \right) \quad \dots\dots\dots(3)$$

$$K^2 = \frac{g^2}{l^2 + m^2 + n^2} \quad \dots\dots\dots(4)$$

The acceleration due to gravity at the location of the experiment was used for the determination of K . In stationary mode, the only acceleration it feels is a 1 g acceleration level in vertical direction. The calibration procedure confirms an average acceleration level of 18.28 mg (milli g is one thousandth of g) along all three directions \underline{l} , \underline{m} and \underline{n} . Also, with the knowledge of angles a , b and c before and after the experimental vibration test the computation could be corrected using the program for miniature variations if exist.

Estimation of the power spectral density (PSD) of the acceleration time series

The vibration data (acceleration time series data) obtained with the Steval accelerometer were analyzed using Discrete Fourier Transformation (DFT) for the estimation of the Power Spectral Density (PSD) of the vibration. Many methods have been discussed in the statistical literature for the estimation of spectra and spectral densities. Of them, the method that has found the widest application in engineering and experimental physics; the “Overlapping Segmented Averaging of Modified Periodogram method” was used in this study for spectral analysis. This method is attributed to Welch and is also known as WOSA or Welch Overlapped Segmented Average (Heinzel et al., 2002, Welch, 1967). Welch method with its default Hamming window of 50% overlap was employed with the sampling rate of 100 Hz.

Power spectral density (PSD) describes how the power of the time series signal is distributed with the frequency. Simply, when a phenomenon is associated with a range of frequencies, the PSD curve indicates frequency/frequencies at which maximum energy is transferred.

Acceleration Power Spectral Density is simply the (overall acceleration level)² divided by the bandwidth (Irvine, 2000). Since a very large range of PSD can be represented by a convenient number, the logarithmic ratio – Decibel – is often used selecting a reference level of acceleration. An acceleration of 0 dB implies the acceleration of interest is equal to the reference level. For the comparison work of acceleration with certain reference level, the PSD is much more conveniently expressed in dB/Hz (Aster and Borchers, 2008).

Vibration simulator

For the simulation of vertical vibration effects in the lower frequency region, (i.e. 2 Hz to 20 Hz), an electro-dynamic vibrator was fabricated using locally available resources. The function of the vibrator is based on the unbalance of rotating masses (Figure 2)

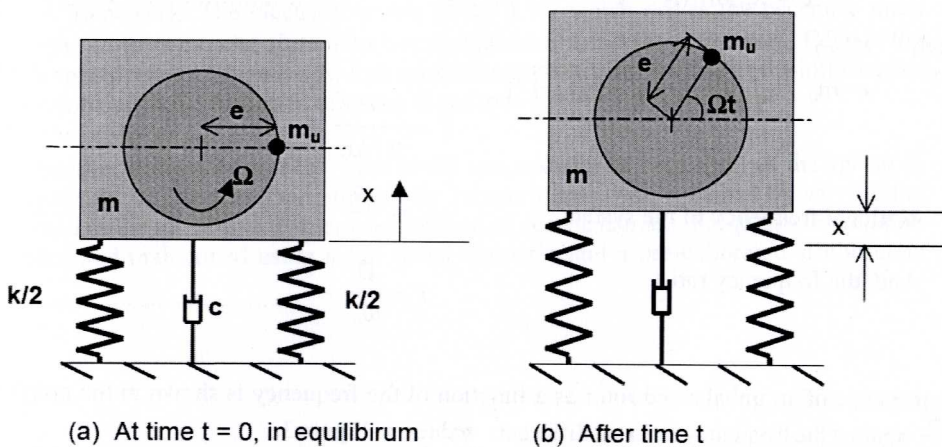


Figure 2. Vibration acceleration produced due to rotation of eccentric mass

A mass of m_u which is eccentrically attached to a rotating uniform disc acts as the mass of unbalance, or commonly referred to as the “eccentric mass”. The eccentricity, or the distance to the eccentric mass from the axis of rotation, is e . The total vibrating part which has a mass m is supported on a spring & dashpot system. The spring constant is k and the damping constant of the dashpot is c . The eccentric mass along with the disc is set to rotate at a constant angular velocity Ω . The displacement of the total vibrating system from its reference level is x . The equation of the motion is then,

$$-kx - c \frac{dx}{dt} = (m - m_u) \frac{d^2x}{dt^2} + m_u \frac{d^2}{dt^2}(x + e \sin \Omega t) \quad \dots\dots\dots(5)$$

$$-kx - c \frac{dx}{dt} = (m - m_u) \frac{d^2x}{dt^2} + m_u \frac{d^2}{dt^2}(x + e \sin \Omega t) \quad \dots\dots\dots(6)$$

This is the same form as the equation of motion for damped forced vibration.

$$\text{i.e. } m\ddot{x} + c\dot{x} + kx = F_0 \sin \Omega t \quad \dots\dots\dots(7)$$

The excitation is due to the applied force F_0 which is $(m_u \Omega^2 e)$. This is the centripetal force produced by the rotating eccentric mass m_u and it acts towards the centre of rotation. If the rotor is well balanced, then e becomes zero and hence the force never exists. The centripetal force $(m_u \Omega^2 e)$ rises up with the eccentric mass m_u , angular frequency Ω and the eccentricity e .

Looking for a solution in the form of

$$x = X_0 \sin(\Omega t - \varphi) \quad \dots\dots\dots(8)$$

We get, $X_0 m = \frac{(r)^2}{\sqrt{(1 - (r)^2)^2 + [2\xi(r)^2]}}$ (9)
where $e m_u$

$$\xi = \frac{c}{2\sqrt{km}} \quad \dots\dots\dots(10)$$

Natural frequency of the system $\omega_n = \sqrt{\frac{k}{m}} \quad \dots\dots\dots(11)$

And, the frequency ratio $r = \frac{\Omega}{\omega_n} \quad \dots\dots\dots(12)$

The response of an unbalanced rotor as a function of the frequency is shown in the graph of $\frac{X_0}{e} \frac{m}{m_u}$ against the frequency ratio r at different values, in Figure 3.

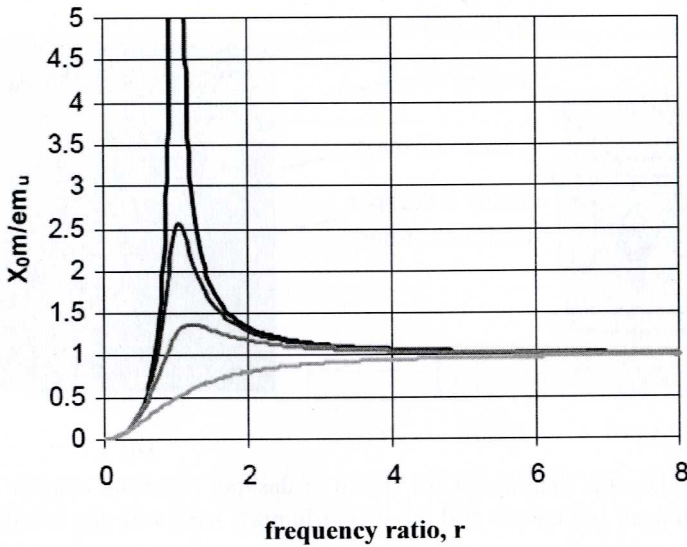


Figure 3: Response of the unbalanced rotor as a function of the frequency ratio r (<http://www.tech.plym.ac.uk>).

Fabrication of the Laboratory Vibration Simulator

Using the principle mentioned above, a metal framework (to be used as the vibrator platform) was hinged at one edge so that it could rotate in a vertical plane about the hinge. Motion of the framework was then restricted to a periodic oscillatory motion having few centimeters amplitude in the vertical plane by coupling the spring & dashpot combination at the opposite edge of the framework. The electrical motor (≈ 0.7 kW) which drives the eccentric mass attached to the uniform circular aluminum disc was fastened under the framework. Edge of the framework opposite to the hinge is now free to execute vertical vibration under the influence of the rotating unbalance and the action of spring & dashpot.

A shock absorber designed for motor bike could successfully be employed as the spring & dashpot assembly. The required variation of the eccentric mass was obtained by varying the mass attached to the aluminum disc provided range of eccentric mass. Frequency of rotation was adjusted and maintained using a fan speed regulator and a pre-calibrated stroboscope (Figure 4).

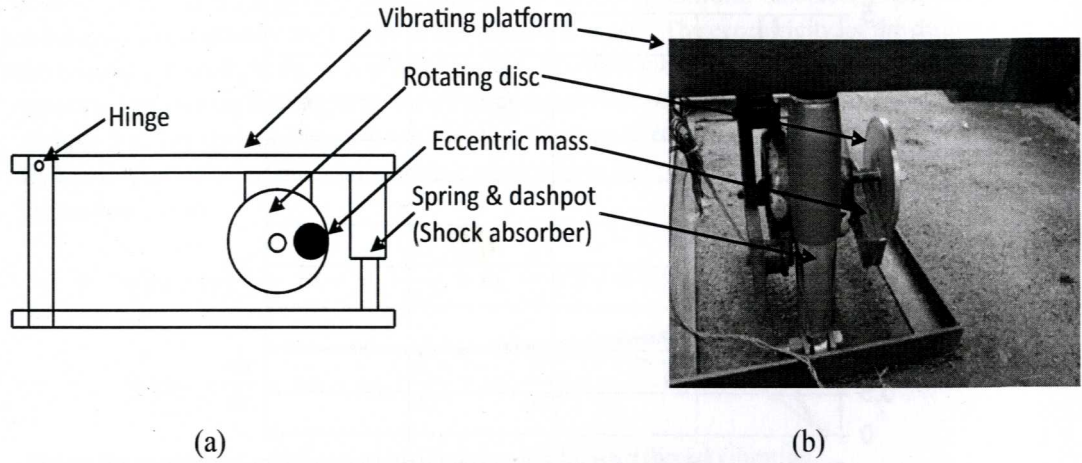


Figure 4: (a) Schematic diagram of the spring & dashpot assembly coupled at the edge opposite to the hinged framework and the eccentric mass used with the locally fabricated vibrator.
(b) Photograph showing essential parts of the locally fabricated vibrator.

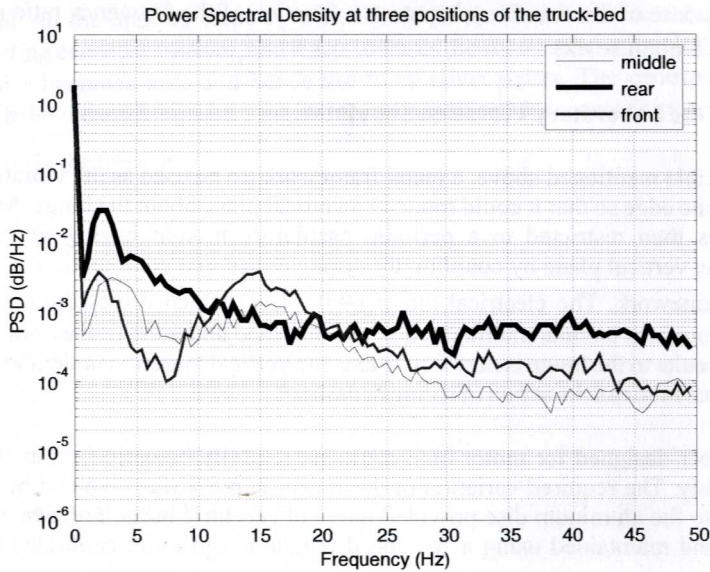


Figure 5: Average of the maximum vertical vibration acceleration (PSDmax) produced at front, middle and rear positions of the empty truck bed

Maximum PSD levels of the truck were registered at lower frequencies (particularly below 10 Hz) and the average of the maximum PSD level of the vertical vibration acceleration produced by the truck was found to be below 0.1 dB/Hz (see Figure 6). Hence, as a representative value, the vibration frequency of 7 Hz was selected for further investigations using the laboratory

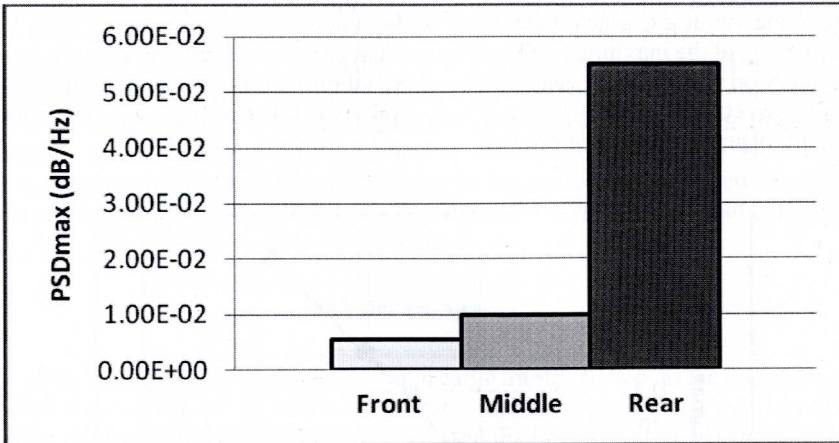


Figure 6: Average of the maximum PSD of the vertical vibration acceleration levels produced at actual road transportation of fruits & vegetables by truck.

Results

Vertical vibration acceleration of the truck

Mitsubishi Canter truck models FE535B6R and FE635E6R were used (Tire inflation air pressure front 65 psi; rear-inner 55 psi; rear-outer 65 psi). The distribution of the vibration acceleration at the front, middle and rear positions along the lengthwise symmetry axis of the empty truck bed when the truck was moving at a speed of 20 kmh^{-1} on fair road rated at Present Serviceability Rating PSR 2 to 3 (or International Roughness Index IRI 3.2 to 2 mm/m) is shown in the Figure 5. Only at 15 Hz the front side of the empty truck registered higher vibration acceleration than that of its rear side; however, the corresponding peak faded away with the loading of the truck. The peak might have caused by resonance of some part of the truck. Figures show that the power spectral density (PSD) of the vibrations generated by the truck bed is high at frequencies below the 10 Hz, in both the empty and loaded truck (Ranatunga et al., 2010).

The operating frequency, eccentric mass and the loaded-weight of the vibration simulator were found to be the effective parameters of the magnitude of the generated vertical vibration acceleration level. Since the critical region of frequency that damages fruits and vegetables, lies below 10 Hz, the vibrator characteristics were further analyzed at the frequency 7 Hz. Figure 7 shows the average of the maximum PSD of the vertical vibration acceleration levels generated at the laboratory on varying the eccentric mass of the vibrator (with no load; at frequency 7 Hz). By selecting the eccentric mass between 200 g – 300 g, the vibrator (no load) can generate the PSD levels met at actual road transportation.

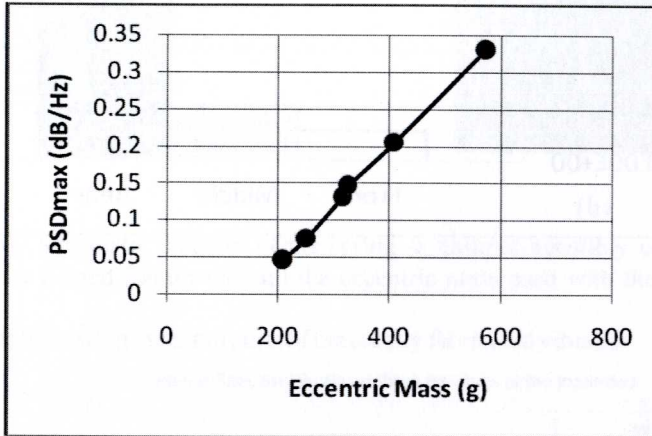


Figure 7: Variation of the PSDmax of the vertical vibration acceleration generated at the laboratory on varying the eccentric mass of the vibrator (no load; frequency 7 Hz).

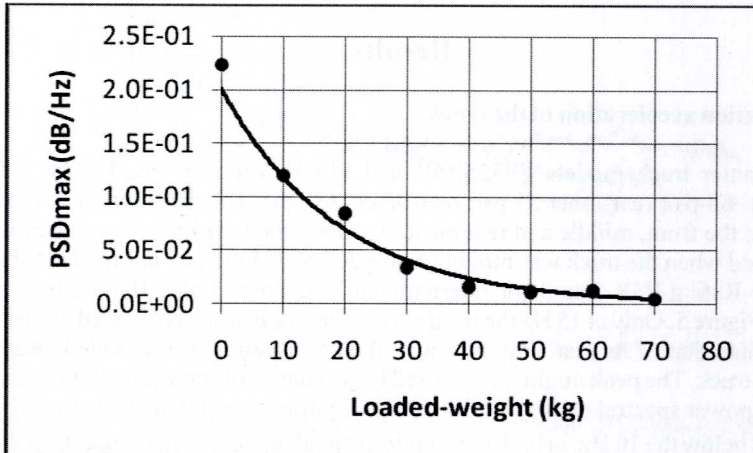


Figure 8: Variation of the PSDmax of the vertical vibration acceleration generated at the laboratory on varying the loaded-weight of the vibrator (eccentric mass 400 g; frequency 7 Hz)

It is common observation that the vibration acceleration decreases with increasing payload in vehicular road transportation. The validity of the phenomenon was tested at the laboratory by varying the loaded-weight of the vibrator. Figure 8 shows the variation of the average of the maximum PSD of the vertical vibration acceleration levels on varying the loaded-weight of the vibrator (at eccentric mass 400 g; at frequency 7 Hz). The range of vertical vibration acceleration levels of truck from 0.5×10^{-3} dB/Hz to 2.0×10^{-1} dB/Hz could successfully be simulated using a range of loaded-weight from 0 to 70 kg on the vibrator platform (compare the Figure 6 for the truck vibration with the Figure 8 for the laboratory vibrator characteristics). By selecting the loaded weight between 15 kg to 60 kg, the vibrator (at eccentric mass 400 g) could generate the PSD levels produced by the front middle and rear sides of the truck at actual road transportation.

Discussion

In view of studying the vibration effects present in cargo transportation, as the first step a suitable low-cost but state of the art IC vibration sensor – the accelerometer – was identified and calibrated for the frequency range of interest. Though the peak vibration acceleration levels at the truck-bed is frequently found within the range 1 to 5 Hz, it developed into a PSD pattern rather having distorted peaks at a higher frequency range, usually between 5 to 10 Hz. The behaviour is similar to that observed by Hinsch (Hinsch et al., 1993). Further, the PSD peaks reported by many authors range to a broad band of frequency between 1 to 15 Hz (Brown et al., 1993, Chonhenchob et al., 2009, Craig et al., 1992, Fischer et al., 1992, Ishikawa et al., 2009, Slaughter et al., 1993, Timm et al., 1998, Van-Zeebroeck et al., 2006). Peak PSD levels observed in this study were found to occur within the frequency range below 10 Hz and it was selected 7 Hz to be the representation for the laboratory simulation of the truck vibration.

Peak PSD level rises up from the front to the rear, horizontally along the truck-bed. Average of the maximum PSD levels produced by the truck at the said frequency interval ranged below 0.1 dB/Hz. The PSD levels of the truck decline with increasing payload. Hence, the laboratory simulation of a PSDmax level of 0.1 dB/Hz serves the purpose.

Parameters of the fabricated vibration simulator, i.e. frequency, eccentric mass, loaded-weight and damping characteristics were adjusted in such a way that the vibration acceleration levels simulated are similar to those of the actual road transportation by truck. PSDmax rises up with the eccentric mass but drops down with the loaded-weight. If the loaded-weight of the simulator need be increased, then the consequent drop in PSDmax can be compensated and maintained at a desired level by increasing the eccentric mass. The fabricated vibration simulator with eccentric mass 400 g produces the range of PSDmax levels of interest of this study when the loaded-weight varied from 15 kg to 60 kg. Since the simulated PSDmax level was found to drop-down exponentially with the loaded-weight, it can successfully be adjusted by varying the eccentric mass and loaded-weight to match the vibration levels of the truck (front, middle or rear) effective at the actual road transportation.

Acknowledgements

Authors acknowledge the financial support from the National Science Foundation under the research grant RG/2007/E/01.

References

- Aster, R. and Borchers, B. (2008) Time series / Dataprocessing and analysis (MATH 587 / GEOP 505). Barchi, G. L., Berardinelli, A., Guarnieri, A., Ragni, L. and Fila, C. T. (2002) Damage to loquats by vibration-simulating intra-state transport. *Biosystems Engineering*, 82(3), 305-312.
- Berardinelli, A., Donati, V., Giunchi, A., Guarnieri, A. and Ragni, L. (2005) Damage to pears caused by simulated transport. *Journal of Food Engineering*, 66, 219-226.
- Brown, G. K., Schulte, N. L., Timm, E. J., Armstrong, P. R. and Marshall, D. E. (1993) Reduce apple bruise damage. *Tree Fruit Postharvest Journal*, October 4(3), 6-10.
- Cann, A. P., Salmoni, A. W. and Eger, T. R. (2004) Predictors of whole-body vibration exposure experienced by highway transport truck operators. *ERGONOMICS*, 47(13), 1432-1453.
- Chonhenchob, V., Sittipod, S., Swadsee, D., Rachtanapun, P., Singh, S. P. and Singh, J. (2009) Effect of truck vibration during transport on damage to fresh produce shipments in Thailand. *Journal of Applied Packaging Research*, Vol. 3, No. 1, 27-38.
- Craig, W. L., Woolsey, M. D., Ashby, B. H. and Fischer, D. F. (1992) Simulated In-transit vibration damage to fresh market Raspberries. *Journal of Food Distribution Research*, June 1992, 69-70.
- Fischer, D., Craig, W. L., Watada, A. E., Douglas, W. and Ashby, B. H. (1992) Simulated in-transit vibration damage to packaged fresh market grapes and strawberries. *Applied Engineering in Agriculture*, 8(3), 363-366.
- Heinzel, G., Rudiger, A. and Shilling, R. (2002) Spectrum and spectral density estimation by the Discrete Fourier Transform (DFT), including a comprehensive list of window functions and some new flat-top windows. Hannover, Max-Planck Institut für Gravitationsphysik (Albert-Einstein Institut).
- Hinsch, R. T., Slaughter, D. C., Craig, W. L. and Thompson, J. F. (1993) Vibration of fresh fruits and vegetables during refrigerated truck transport. *Trans. ASAE*, 36, 1039-1042.
<http://www.tech.plym.ac.uk>

Irvine, T. (2000) Power spectral density units [g²/Hz]. Vibration.com.

shikawa, Y., Kitazawa, H. and Shiina, T. (2009) Vibration and shock analysis of fruit and vegetables transport Cherry transport from Yamagata to Taipei—. JARQ 43 (2), 129-135.

Pauly, W. (2008) Introduction to vibration testing (part 2). ERI News. Santa Barbara, Equipment Reliability Institute.

Ranatunga, C. L., Jayaweera, H. H. E., Suraweera, S. K. K., Wattage, S., Ruvinda, K. K. D. L. and Ariyaratne, T. R. (2010) Vibration effects at vehicular road transportation. IPSL Annual Technical Sessions (26). Colombo, Institute of Physics, Sri Lanka.

Slaughter, D. C., Hinsch, R. T. and Thompson, J. F. (1993) Assessment of vibration injury to Bartlett Pears. American Society of Agricultural Engineers VOL. 36(4), 1043-1047.

Steval (2006) Theory of Operation - Steval Application Note AN 2335. Steval Microelectronics.

Timm, E. J., Bollen, A. F., Rue, B. T. D. and Woodhead, I. M. (1998) Apple damage and compressive forces in bulk bins during orchard transport. Applied Engineering in Agriculture, 14(2), 165-172.

Usuda, H., Ishikawa, Y., Nakamura, N., Roy, P., Nei, D., Orikasa, T., Satake, T. and Shiina, T. (2008) Design Method of Power Spectrum Density Profile for Random Vibration Test Based upon S-N Curve. ASABE Paper No. 08 - St. Joseph, Mich.: ASABE Annual International Meeting.

Van-Zeebroeck, M., Tijssens, E., Dintwa, E., Kafashan, J., Loodts, J., Baerdemaeker, J. D. and Ramon, H. (2006) The discrete element method (DEM) to simulate fruit impact damage during transport and handling: Case study of vibration damage during apple bulk transport. Postharvest Biology and Technology, 41, 92-100.

Vursavus, K. and Ozguven, F. (2004) Determining the effects of vibration parameters and packaging method on mechanical damage in Golden Delicious apples. Turk. J. Agric. for, 28, 311-320.

Welch, P. D. (1967) The use of Fast Fourier transformation of power spectra: A method based on time averaging over short, modified periodograms. IEEE Trans. Audio and Electroacoust., AU-15, 70-73.

Zhou, R., Su, S., Yan, L. and Li, Y. (2007) Effect of transport vibration levels on mechanical damage and physiological responses of Huanghua pears (*Pyrus pyrifolia* Nakai, cv. Huanghua). Postharvest Biology & Technology, 46, 20-28.